

## Article

# Experimental Study of a Loop Heat Pipe with Direct Pouring Porous Wick for Cooling Electronics

Bing Cai <sup>1</sup>, Weizhong Deng <sup>1</sup>, Tong Wu <sup>1</sup>, Tingting Wang <sup>1</sup>, Zhengyuan Ma <sup>1</sup>, Wei Liu <sup>1</sup>, Lei Ma <sup>2,\*</sup> and Zhichun Liu <sup>1,\*</sup> 

<sup>1</sup> School of Energy and Power Engineering, Huazhong University of Science and Technology, Wuhan 430074, China; m202071084@hust.edu.cn (B.C.); m201871167@hust.edu.cn (W.D.); m202071101@hust.edu.cn (T.W.); wttbtdisxback@163.com (T.W.); d202080481@hust.edu.cn (Z.M.); w\_liu@hust.edu.cn (W.L.)

<sup>2</sup> College of New Materials and New Energies, Shenzhen Technology University, Shenzhen 518118, China

\* Correspondence: malei@sztu.edu.cn (L.M.); zcliu@hust.edu.cn (Z.L.)

**Abstract:** A pouring silicate wick was manufactured to explore the influence of process and physical properties on the production and performance of loop heat pipes (LHP). This paper theoretically analyzed the advantages of pouring porous wick and introduced the technology of pouring silicate directly on evaporator. Based on this, the heat transfer performance of copper-methanol LHP system with pouring porous wick was tested under different positions. The results showed that with the input of multiple heat sources, the LHP could start up and maintain a stable temperature from 40 W to 160 W. When the vapor grooves were located above the compensation chamber, it was difficult to start up positively. By adding gravity assistance, the system could obtain more stable liquid supply and vapor flow, so as to realize start up. In the variable heat load test, the LHP showed good adaptability to the change of heat load. The thermal resistance of the system decreased with the increase of heat load. The thermal resistance of the evaporator almost unchanged and was always lower than 0.05 °C/W, which indicated that the pouring porous wick in the evaporator had good heat load matching.

**Keywords:** loop heat pipe; copper-methanol; electronics cooling; pouring porous wick; multiple heat sources



**Citation:** Cai, B.; Deng, W.; Wu, T.; Wang, T.; Ma, Z.; Liu, W.; Ma, L.; Liu, Z. Experimental Study of a Loop Heat Pipe with Direct Pouring Porous Wick for Cooling Electronics. *Processes* **2021**, *9*, 1332. <https://doi.org/10.3390/pr9081332>

Academic Editor: Alfredo Irazzo

Received: 5 July 2021

Accepted: 28 July 2021

Published: 30 July 2021

**Publisher's Note:** MDPI stays neutral with regard to jurisdictional claims in published maps and institutional affiliations.



**Copyright:** © 2021 by the authors. Licensee MDPI, Basel, Switzerland. This article is an open access article distributed under the terms and conditions of the Creative Commons Attribution (CC BY) license (<https://creativecommons.org/licenses/by/4.0/>).

## Highlights

The technology and process of direct pouring porous wick for LHP were introduced. A flat LHP with a pouring silicate wick and three heat sources was fabricated.

The lowest  $R_{LHP}$  was 0.195 °C/W and the  $R_{eva}$  was always below 0.050 °C/W under the heat load from 40 W to 160 W.

When the vapor grooves were located above the compensation chamber, the LHP could start up by gravity assistance.

## 1. Introduction

Loop heat pipe (LHP) is an important device to solve the heat dissipation of high heat flux thermal control system, which has the advantages of high efficiency, strong heat transfer ability and compact structure. It is widely used in aerospace equipment [1], solar energy [2], and power battery thermal management systems [3]. However, its industrial and commercial applications still have much space for improvement due to its high cost and complex fabrication process [4].

As shown in Figure 1, an LHP is composed of evaporator, vapor/liquid line and condenser. The evaporator is the most significant part of LHP whose design and processing are particularly important. For a flat LHP, the selection and assembly of porous wick and

the design of evaporator structure are the determining factors of the stability and efficiency of an LHP [5].

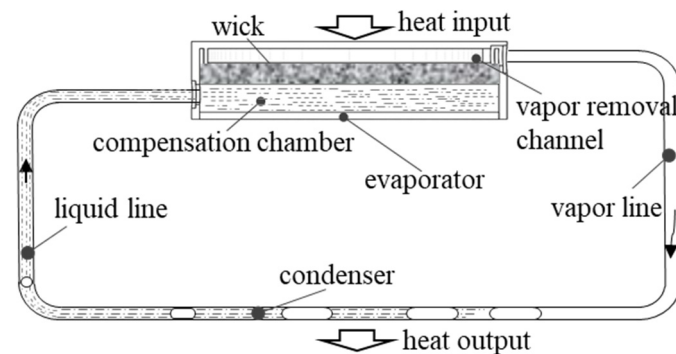


**Figure 1.** LHP's composition and working principle.

At present, the porous wicks widely used in LHPs are mainly fabricated by metal wire mesh [5], foam metal [6], sintered metal powder [7], and so on. Deng et al. [8] used metal wire mesh to make porous wicks in LHP evaporators with a heat dissipation area of  $190 \text{ mm} \times 90 \text{ mm}$ . They used acetone as the working fluid to study the heat transfer performance of the system. Wang et al. [5] experimentally studied the influence of sintered copper powder porous wicks and copper wire mesh porous wicks on the heat transfer performance of LHP. The data showed that the sintered porous wick has a faster start up speed, more stable operation, and lower thermal resistance than metal wire mesh porous wick. Zhou et al. [6] fabricated a multilayer foam metal wick evaporator. Experiments showed that multilayer foam copper has higher thermal conductivity and a smaller effective aperture than foam nickel, shorter start up time, and a lower thermal resistance during operation. Zhang et al. [7] manufactured a biporous wick with nickel powder and constructed a flat-plate LHP with long heat transfer distance to test the performance limit of the biporous wick. The experimental results showed that the maximum heat load was  $110 \text{ W}$  ( $6.6 \text{ W/cm}^2$ ) and the minimum thermal resistance of the LHP was  $0.382 \text{ }^\circ\text{C/W}$ . Ren et al. [9] established an axisymmetric two-dimensional mathematical model to study the influence of heat flux and porous structure parameters on the working state and performance of porous wick, which was instructive for the design of more precise porous wick. Hu et al. [10] used 3D printing technology to make a stainless steel porous wick that could start successfully at a low heat load of  $20 \text{ W}$  ( $2.83 \text{ W/cm}^2$ ) and operated stably in a wide heat load range between  $20 \text{ W}$  and  $160 \text{ W}$  ( $22.63 \text{ W/cm}^2$ ). The minimum LHP thermal resistance was  $0.181 \text{ K/W}$  at a heat load of  $160 \text{ W}$ . Li et al. [11] selected porous  $\text{Si}_3\text{N}_4$  ceramics with monomodal and bimodal pore size distribution as novel wick materials for loop heat pipe. They found that wicks with monomodal pore structure displayed lower liquid uptake capacity and larger filling coefficient in comparison with those with bimodal pore structure. Furthermore, the wicks using working fluid with lower viscosity, larger surface tension and density showed better capillary performance.

In recent years, some other methods of fabricating porous wick have also been applied. The most common type is sintered metal porous wick, owing to its smaller effective pore size and higher thermal conductivity. Direct sintering on the vapor grooves is the most ideal way in which the thermal resistance of heat conduction can be greatly reduced [12,13]. Moreover, the metal mesh porous wick is also widely used, which is easy to make and can be cut directly according to the shape of the evaporator. Additionally, simple porous wick processing method was broadly applied in research [14,15]. However, both the cost and the dimension error requirement of the above two methods are high, especially for the sintered porous wick [4].

In comparison with the aforementioned other methods, pouring porous wick has many advantages. First, the cost of raw materials is very low as the average price of 300 mesh copper powder is 150 RMB/kg, while that of 300–400 mesh silicate is only

2 RMB/kg. We have done a lot of LHP experiments with sintered metal powder wick in our previous studies [13,16,17]. Compared with copper powder, the cost of silicate is only about one-seventieth. At the same time, pouring at ambient temperature does not require additional high temperature equipment. In terms of auxiliary devices, the sintered metal porous wick needs high temperature sintering furnace and reducing gas. From the perspective of the economy, the pouring method will further reduce the cost of manufacturing LHP system. Considering the heat transfer performance of porous wick material, the pouring porous wick is processed by cement, which is mainly composed of silicate and water. The thermal conductivity of cement is within  $2 \text{ W}/(\text{m}\cdot\text{K})$ , while the thermal conductivity of metal sintered porous wick is much greater than this value. According to Maxwell equation:

$$\lambda_E = 2\lambda_S(1 - \varepsilon)/(2 + \varepsilon) \quad (1)$$

where  $\lambda_E$  is effective thermal conductivity of porous materials,  $\lambda_S$  is the thermal conductivity of solid metal and  $\varepsilon$  is the porosity. For example, the porous wick with 60% porosity sintered by copper powder's effective thermal conductivity is about  $117 \text{ W}/(\text{m}\cdot\text{K})$ , which is more than 50 times of that of cement. Therefore, the back heat leakage of LHP can be reduced under the condition of good sealing performance.

For large LHP, the direct pouring method also has the unique advantage that it is not limited by the shape and area of evaporator. When the heat load is given, increasing the heating area can effectively reduce the heat flux, so as to ensure that the electronic equipment works in a safe temperature range. Obviously, the increase of evaporator area limits the structural strength and flatness of sintered porous wick. It can be predicted that direct sintering or pouring on evaporator will be an inevitable trend for large LHPs in the future.

In this paper, a pouring porous wick was designed for the large area LHP. A series of tests were carried out for the LHP with the pouring porous wick. The heat transfer performance of the system was analyzed.

## 2. Design of the LHP

The manufacturing process of pouring porous wick was introduced in article [4] and its flow chart is shown in Figure 2. It is worth noting that the pouring porous wick in article [4] is limited by the mold, which restricts the match with various shapes of evaporator and loses the advantages of pouring method.

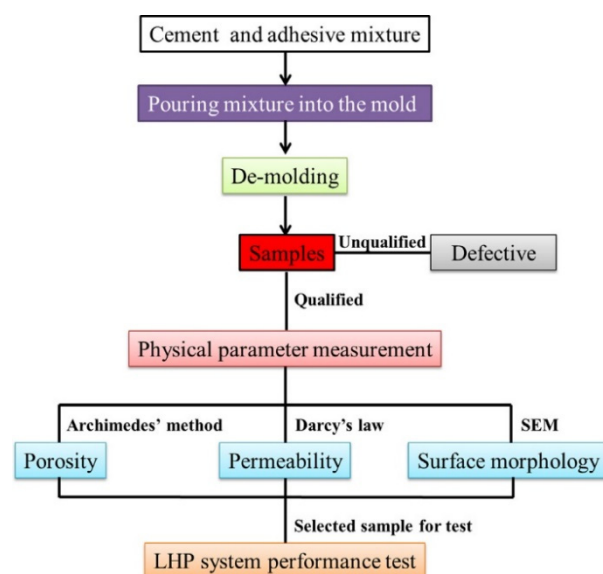
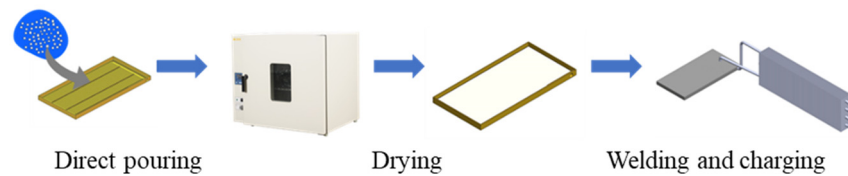
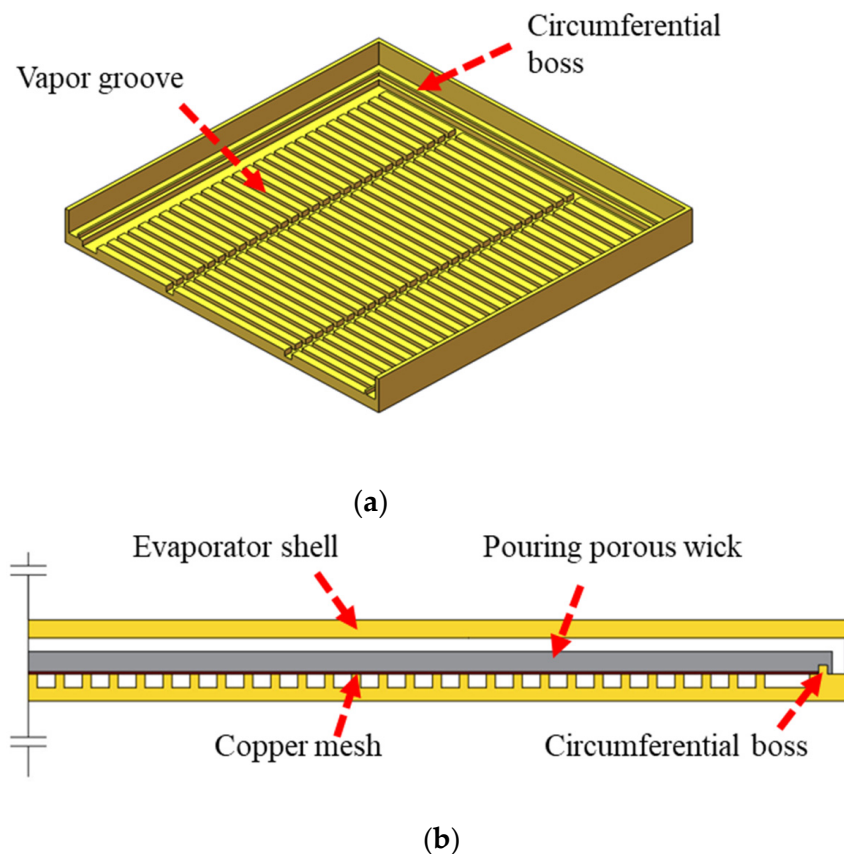


Figure 2. Flow chart of pouring porous wick fabrication by He et al. [4].

However, the production process presented in this paper can be represented as Figure 3 and the structure of the evaporator is shown in Figure 4. The shell of the evaporator is the limiting boundary for the porous wick instead of a mold. Through the circumferential boss set on the peripheral side of the evaporator, the pouring material was tightly combined with the bottom surface of evaporator and the outside of the boss by the effect of gravity settlement and liquid evaporation shrinkage. This could reduce the thermal resistance and improve the sealing performance between the compensation chamber and evaporation area.



**Figure 3.** Production process of the direct pouring LHP.



**Figure 4.** Structure of the evaporator. (a) Half shell of the evaporator (b) Cross-section after pouring.

The specific process is as follows. First, the copper evaporator was cleaned by acetone and the oxide on the surface was removed by acid detergent. The cement was washed by deionized water for more than three times. Then, it was put into the cement paste mixer and stirred for 1 h. To form the vapor grooves effectively, a layer of copper mesh was laid on the heat conducting ribs to prevent the cement from blocking the grooves. If the vapor grooves were blocked, the LHP could not start up in subsequent experiments. The cement was evenly poured on the heat conducting rib of the evaporator. The thickness of the cement should be greater than the height of the circumferential boss to make it completely submerged, so as to form a good sealing between the vapor side and the compensation chamber side. At the same time, make sure that there is enough volume of the compensation chamber. After pouring 72 h, the morphology of the pouring porous

wick is shown in Figure 5. The thickness of the wick was 2.5 mm and the porosity was 40%. After the completion of the pouring, the evaporator was put into the drying oven and the temperature was set at 80 °C for about 10 h. Finally, the evaporator, condenser and pipeline were welded and the LHP system was charged. Methanol was selected as the working fluid with a charge ratio of 70%.



Figure 5. Morphology of the porous wick after pouring 72 h.

The parameters of LHP system are shown in Table 1.

Table 1. Parameters of the LHP.

Evaporator	L/W/H	180/90/9 mm	Groove depth	1.5 mm	Material	Copper
	Groove width	2 mm	Groove number	55	Working fluid	Methanol
Compensation chamber	L/W/H	178/88/1.5 mm				
Porous wick	Porosity	40%	Material	Silicate	Thickness	2.5 mm
Condenser	O/I	6/5 mm	Fin thickness	0.2 mm	Pipe length	1220 mm
Vapor Line	Material	Copper	Length	185 mm	O/I	6/4 mm
Liquid Line	Material	Copper	Length	222 mm	O/I	6/4 mm

### 3. Experimental Setup

#### 3.1. LHP Experimental System

The experimental system mainly included the heating part, condensing device, power controller, and temperature acquisition system. The heating part of the system was composed of three 40 × 40 mm ceramic heating plates, whose power was controlled by a series power controller. A layer of heat conducting silicone grease was coated between the ceramic heating plates and the heating surface of the evaporator to reduce the contact thermal resistance. An air-cooled finned tube condenser with three fans was used in the LHP system. The signal of each T-type thermocouple was collected by the temperature collector, which was converted into the corresponding temperature value by software EsayDaq and stored in the computer. The temperature measurement error of T-type thermocouple was ±0.5 °C. The arrangement of thermocouples and a prototype of the system are shown in Figure 6. H1-H4 were on the heating surface and close to the heating sources. The distance between H1 and H2 was 50 mm, which was equal to that of H3 and H4. The distance between H2 and H3 was 60 mm. CC-wall was on the back of the evaporator, which indicated the temperature of the compensation chamber. Eva-in, eva-out were at the inlet and outlet of the evaporator respectively. Con-in, con-out, con-mid were at the inlet, outlet and middle of the condenser respectively. During the experiment, the heat sources, vapor line and liquid line were wrapped with insulation cotton to reduce the heat exchange with the environment. Two air conditioners were used to control the ambient temperature within 17 ± 1 °C.

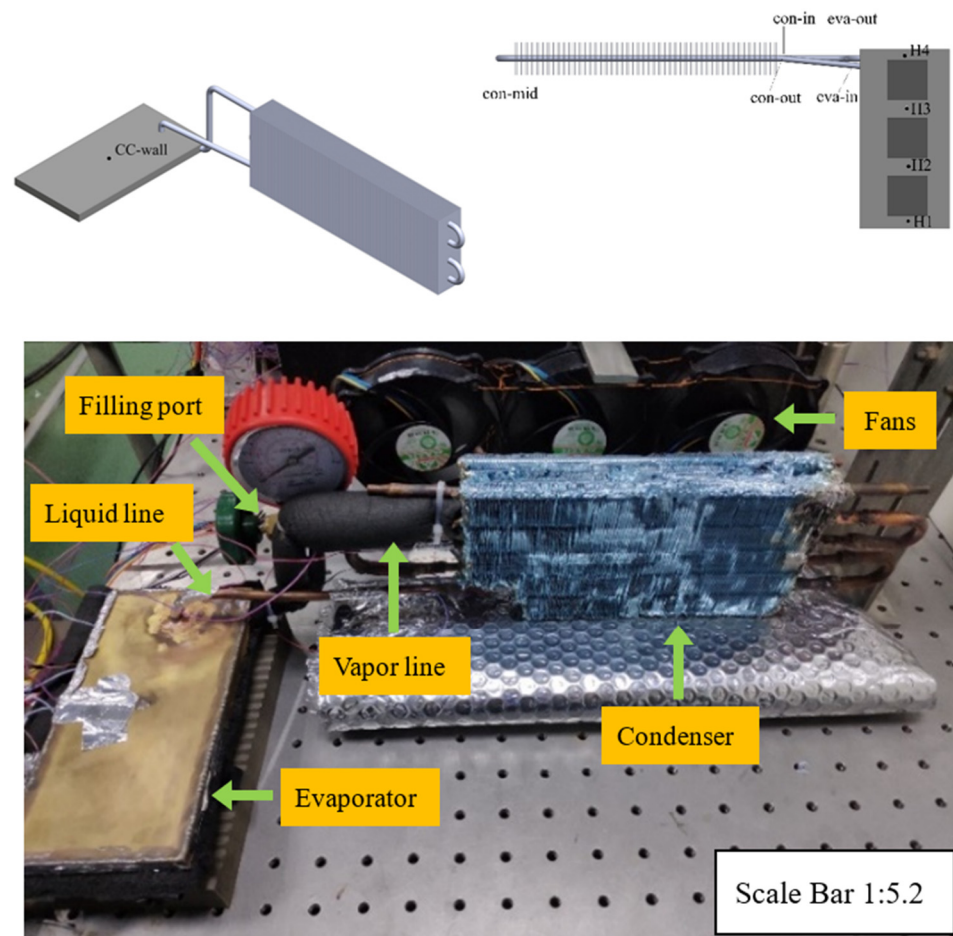


Figure 6. LHP experimental diagram and prototype.

To explore the operation of LHP in different positions, several positions shown in Figure 7 were set for the transient response test of thermal load.  $\Theta$  is the angle between the system and the horizontal plane. Under No.1–No.4 positions, the heat sources were located higher than evaporator, while the heat sources were located lower than evaporator under No.5 and No.6 positions. There was gravity assistance in No.2–No.4 positions' liquid line but it was in the opposite direction inside the evaporator. No.6 position was under unfavorable condition of gravity. No.1 position was a rare position of LHP. The vapor grooves of this position were located above the compensation chamber, which was not conducive to the liquid supply of the porous wick. This problem could be improved by adding a secondary wick [18].

Generally, the circulating power of LHP is provided by the capillary force at the two-phase interface of the porous wick, which greater than the sum of all parts of the system's resistances. The formula is as follows:

$$\Delta p_{cap} > \Delta p_{total} = \Delta p_{groove} + \Delta p_{vl} + \Delta p_{cond} + \Delta p_{ll} + \Delta p_{wick} + \Delta p_g \quad (2)$$

However, the premise of this theory is that the fluid must form a continuous loop in the system, especially in the liquid or multiphase region.

According to the existing research, the start up process is mainly as follows. First, the heat load is loaded on the heating surface of the evaporator, and the vapor in the evaporator pushes the liquid working fluid in the vapor line into the condenser. After heat exchange, it becomes subcooled liquid and flows back to the compensation chamber. Then the compensation chamber supplies the liquid to the porous wick. The system can be stabilized only after each step of the process is successfully implemented.

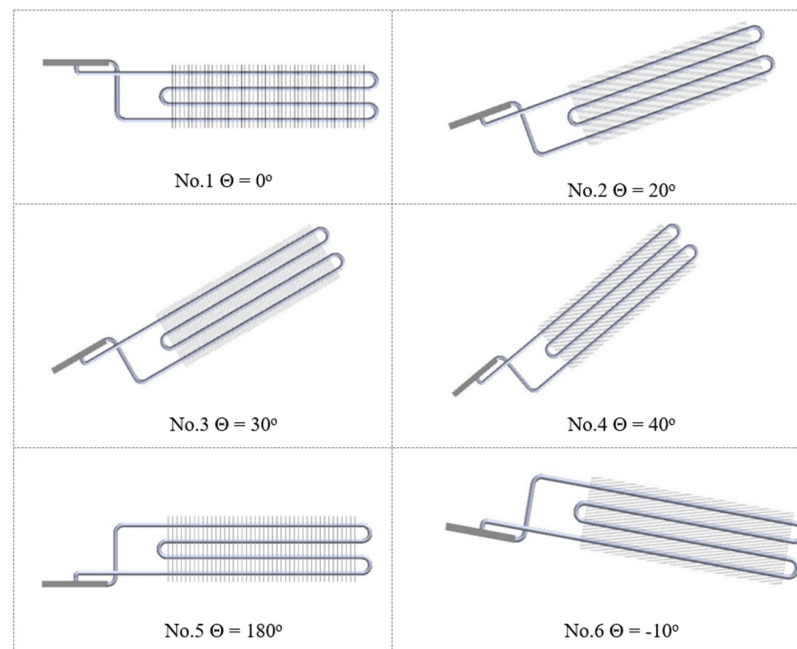


**Figure 7.** Diagram of the LHP under different positions.

### 3.2. Data Processing Method

The main physical parameters in the experiment include the input power  $Q$ , the temperature of each point  $T_i$ , the heat flux of heating area  $q$ , the system thermal resistance  $R_{LHP}$ , the evaporator thermal resistance  $R_{eva}$  and the condenser thermal resistance  $R_{con}$ . The input power  $Q$  was controlled by the power regulator. The heat sources were ceramic heating plates, which were pressed with the heating surface and wrapped with insulation cotton so as to diminish the heat loss.

The total heating area of the heat sources is  $A$ . The heat flux of evaporator heating surface can be calculated as:

$$q = Q/A \quad (3)$$

The calculation formulas of thermal resistances are as follows:

$$R_{LHP} = (T_e - T_c)/Q \quad (4)$$

$$R_{eva} = (T_e - T_{e,out})/Q \quad (5)$$

$$R_{con} = (T_c - T_a)/Q \quad (6)$$

where  $T_e$  is the evaporator wall temperature and is considered to be constant after the system operates stably,  $T_{e,out}$  is the evaporator outlet temperature,  $T_c$  is the average temperature of the condenser inlet and outlet which is calculated by  $T_c = (T_{con,in} + T_{con,out})/2$ ,  $T_a$  is the ambient air temperature.  $T_e$  was considered to be constant.

## 4. Experimental Results and Analysis

### 4.1. Start Up Performance of Position No.1 (Heat Input Was Terminated at 480 s)

In No.1 position, the working fluid could not be continuously pumped to the phase transition interface by the porous wick, which led to the continuous rise of evaporator temperature. As shown in Figure 8, under the heat input of 120 W, the evaporator temperature reached 100 °C at about 260 s with no trend of stability. When the temperature of heating surface reached 140 °C, the heat input was terminated.

The experimental results showed that there was a great temperature difference on the heating surface of the evaporator since it was difficult for the porous wick to replenish the liquid needed for evaporation. The evaporator's area was large and had three heat sources. The liquid inlet was close to H4 point but far away from H1. Moreover, our pervious tests

before experiments showed that the permeability of the pouring porous wick was lower than that of the metal sintered porous wick, which also inhibited the liquid supply away from the inlet of the compensation chamber.

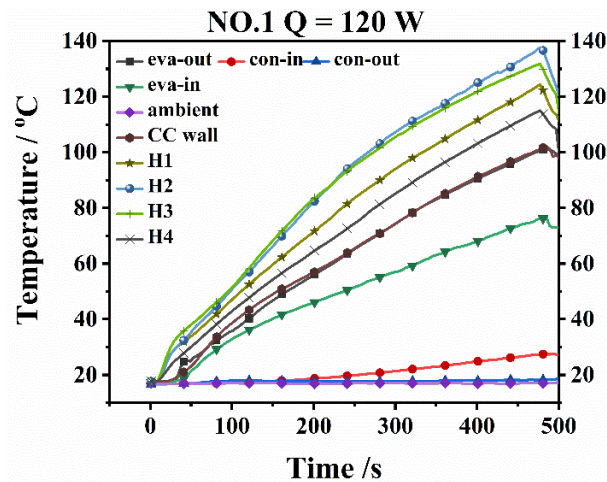


Figure 8. Temperature response during startup process of No.1 position at 120 W.

#### 4.2. Start Up Performance of Position No.2 (Heat Input Was Terminated at 1480 s and 650 s)

In No.2 position, the condenser was higher than the evaporator, and the angle between the system and the horizontal plane was  $20^\circ$ . This position could increase the gravity assistance, which was conducive to the flow of vapor. At the same time, it was beneficial for the liquid at the inlet of the compensation chamber to enter the porous wick along the evaporator shell.

As shown in Figure 9, the LHP of No.2 position still failed to start at 80 W and 120 W heat load. However, compared with No.1 position, the evaporator outlet temperature and evaporator inlet temperature of No.2 position rose synchronously at first, which showed the working fluid in the compensation chamber was in two-phase state. Meanwhile, the rising condenser inlet temperature proved that the vapor entered the condenser through the vapor line. After a while, the condenser inlet temperature suddenly decreased and the condenser outlet temperature increased sharply before it decreased soon. This indicated that the system tended to operate in reverse direction, but the driving force of reverse flow was not enough to maintain the continuity of the working medium. At the heat load of 80 W and 120 W, the condenser outlet temperature began to drop at 400 s and 273 s, respectively. When the condenser outlet temperature and condenser inlet temperature intersected again, the evaporator inlet temperature began to drop, which indicated the working fluid in the liquid line entered the compensation chamber. However, the heating surface temperature and the evaporator outlet temperature did not decrease, because the flow of the working fluid was discontinuous and the liquid in the compensation chamber could not be supplied to the porous wick for evaporation. The temperature of heating surface had no trend of stability, so the system finally failed to start.

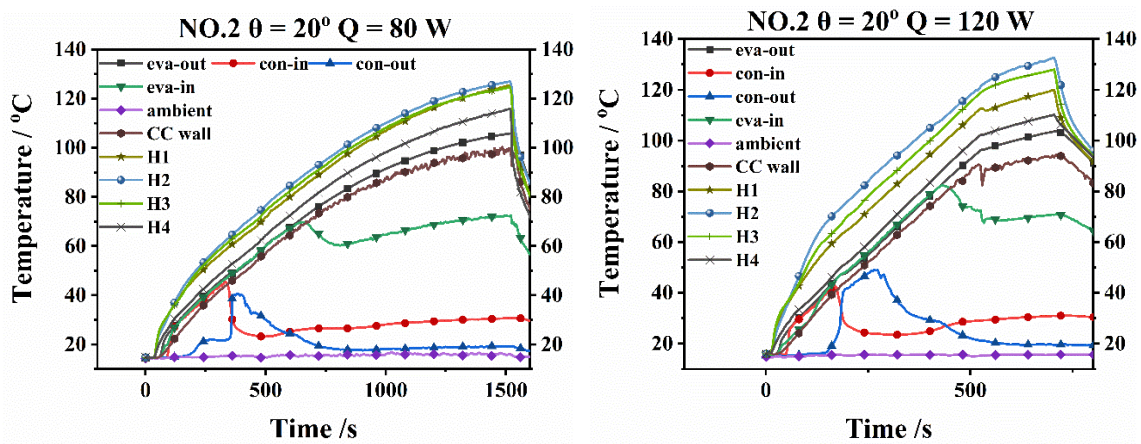


Figure 9. Temperature response during start up process of No.2 position at 80 W and 120 W.

#### 4.3. Start Up Performance of Position No.3 and No.4

Increasing the tilt angle to  $30^\circ$ , the system could start and the temperature of each point was within a certain range. As shown in Figure 10, the system started up smoothly at 80 W but the reverse flow occurred obviously. The highest vapor temperature was  $48^\circ\text{C}$  and the heating surface temperatures of the evaporator were below  $80^\circ\text{C}$ . However, the temperature difference between H1–H4 points was still large. The temperature of H1 was about  $23^\circ\text{C}$  higher than that of H4. On the other hand, the temperatures of H1–H3 were much higher than that of vapor. This was not caused by the excessive contact thermal resistance, but due to the shortage of phase change working fluid supply.

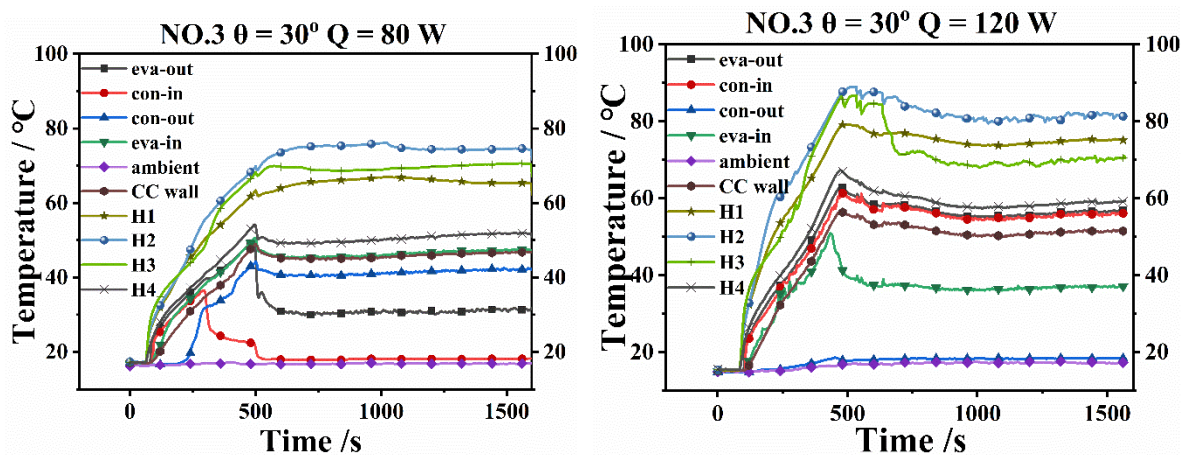


Figure 10. Temperature response during start up process of No.3 position at 80 W and 120 W.

At 120 W heat load, it was worth noting that the temperature of H3 decreased suddenly after starting up to the maximum temperature of  $86^\circ\text{C}$ . It finally stabilized around  $70^\circ\text{C}$  and gradually tended to the temperature of H4. The reason for this phenomenon was that the higher heat load increased the vapor's mass flow rate and the reflux liquid's velocity in the circulation process. The compensation chamber could supply more liquid to the porous wick so that the temperature of H3 decreased.

Increasing the tilt angle to  $40^\circ$ , the start up process of No.4 position is shown in Figure 11. Compared with the No.3 position, there were zigzag temperature fluctuations at 80 W heat load, which is a common phenomenon in low heat load start up of flat LHP.

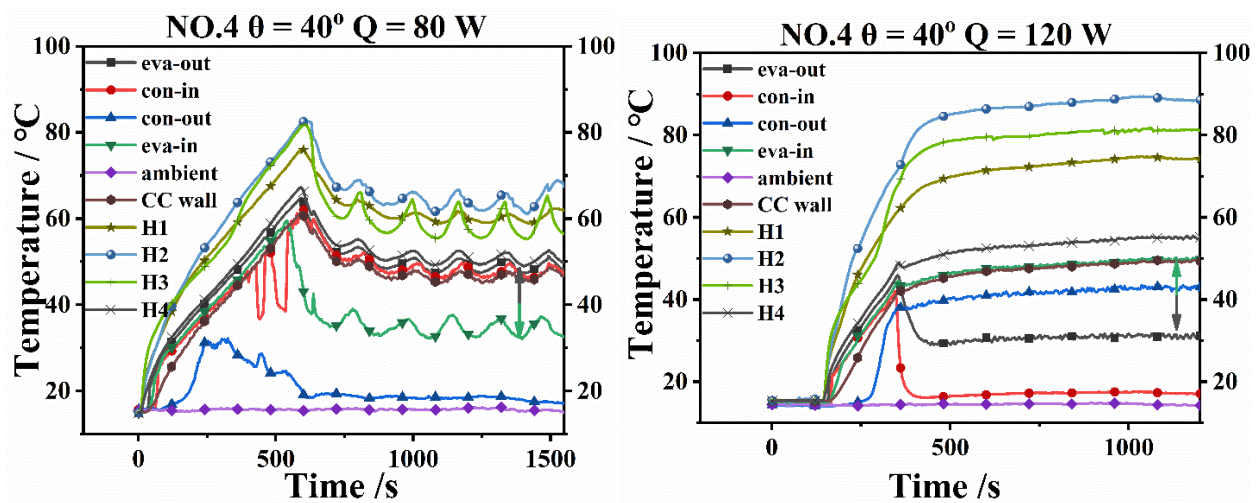


Figure 11. Temperature response during start up process of No.4 position at 80 W and 120 W.

Generally, due to heat leakage, the condenser inlet temperature will be slightly lower than the evaporator outlet temperature. There is a certain heat transfer temperature difference between the condenser outlet temperature and the refrigerant temperature. The evaporator inlet temperature is close to the condenser outlet temperature. If the heat leakage of the evaporator is large, the inlet temperature will also rise.

The experimental results showed that the condenser outlet temperature was lower than the condenser inlet temperature at 80 W. The difference between the condenser outlet temperature and the ambient temperature was not more than 2 °C under the condition of air cooling.

In fact, when the heat load was 80 W, the condenser outlet temperature tried to rise but decreased to ambient temperature finally. The reason is that the condenser outlet temperature rose before the condenser inlet temperature was that the evaporator was closer to the condenser outlet than the condenser inlet. That meant the flow resistance of vapor from evaporator outlet to condenser outlet was lower. The vapor first arrived at condenser outlet but could not push up the liquid in the condenser. Thus, the condenser outlet temperature increased. With the accumulation of the vapor at the condenser inlet, the pressure raised and pushed the system in a positive direction, and the condenser outlet temperature decreased to close to the ambient temperature. Since the condenser was air-cooled, the temperature fluctuations of each point were more intense in this process.

However, when the heat load was 120 W, it was unreasonable that the condenser outlet temperature was higher than the condenser inlet temperature. It could be inferred that the system was in reverse flow. In this regard, the vapor generated in the compensation chamber and entered the condenser for cooling through the liquid line.

This kind of phenomenon is rare in articles, because the position of LHP with the vapor grooves higher than the compensation chamber is rarely studied. This situation was a self-adjustment of the system because the compensation chamber could not supply liquid in time. The liquid supply to the porous wick was not enough, so the continuous heat input made the liquid evaporate in the compensation chamber and generated vapor. Since it was difficult for the vapor to pass through the porous wick, the vapor was cooled after converging through the liquid line to the condenser, and the circulation was established.

Comparing the evaporator outlet temperature of No.1–No.4 positions, it could be seen that the increase of the tilt angle effectively shortened the time for vapor flowing out of the evaporator. The larger the angle, the shorter the time for vapor to converge and flow out of the evaporator.

#### 4.4. Start Up Performance of Position No.5 and No.6

No.5 position was a common position of flat LHP. The condenser was located higher than the evaporator, so its gravity-assisted effect was more obvious. When the heat load was 40 W, 80 W, 120 W, and 160 W, the maximum temperature of heating surface was 43.7 °C, 64.5 °C, 84.5 °C and 108.8 °C. As shown in Figure 12, there was no reverse flow occurring in the system, which further showed that the relative position of vapor grooves and compensation chamber in the LHP had an important influence on the start up and operation of the system. However, there was still a large temperature difference on the heating surface of the evaporator with three heat sources. The large temperature difference was caused by many factors, including uneven distribution of heat sources, poor liquid supply of porous wick, large thermal contact resistance between ceramic heating plates and evaporator, and so on.

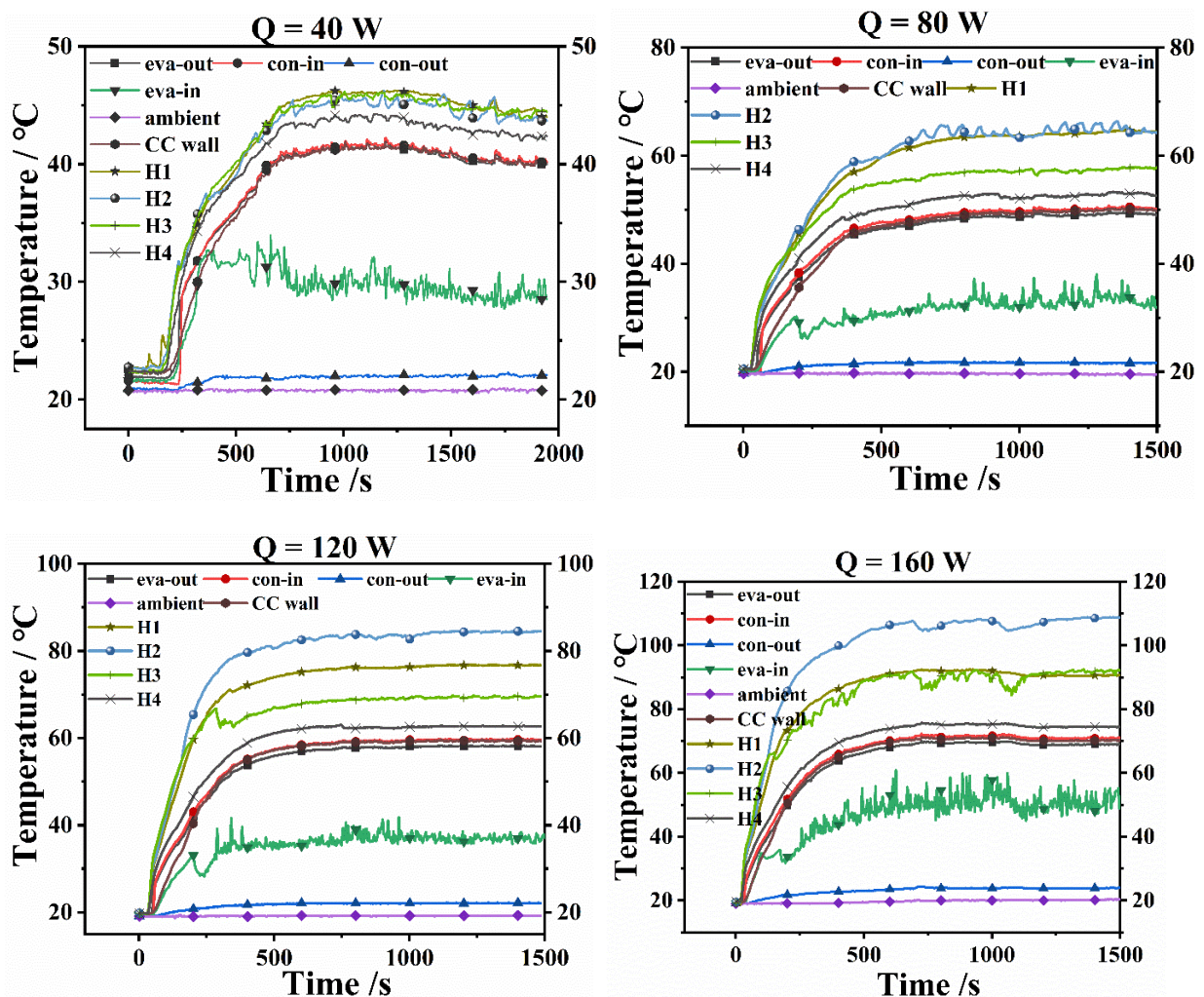


Figure 12. Temperature response during start up process of No.5 position at 40 W, 80 W, 120 W and 160 W.

The No.6 position was under unfavorable condition of gravity, but the system still started up successfully. As shown in Figure 13, at the same 120 W power, the temperature of heating surface was about 20 °C higher than that of the No.5 position. However, the temperature uniformity was improved. It was obvious that the temperature difference between H1–H3 points on the heating surface was very small, but the temperature of H4 point was about 20 °C lower than that of the other three points. The reason was that H4 point was closest to the evaporator inlet, and the working fluid reached H4 first. After the liquid entered the compensation chamber of the evaporator, it was divided into two parts. One part evaporated in the capillary core near H4 point. The other part flowed to the other

side of the compensation chamber and evaporated in the capillary core far away from H4 point. Then the vapor left from the evaporator outlet together. It could be inferred that there was more liquid evaporated near H4 point so that the temperature of H4 was much lower than that of H1–H3.

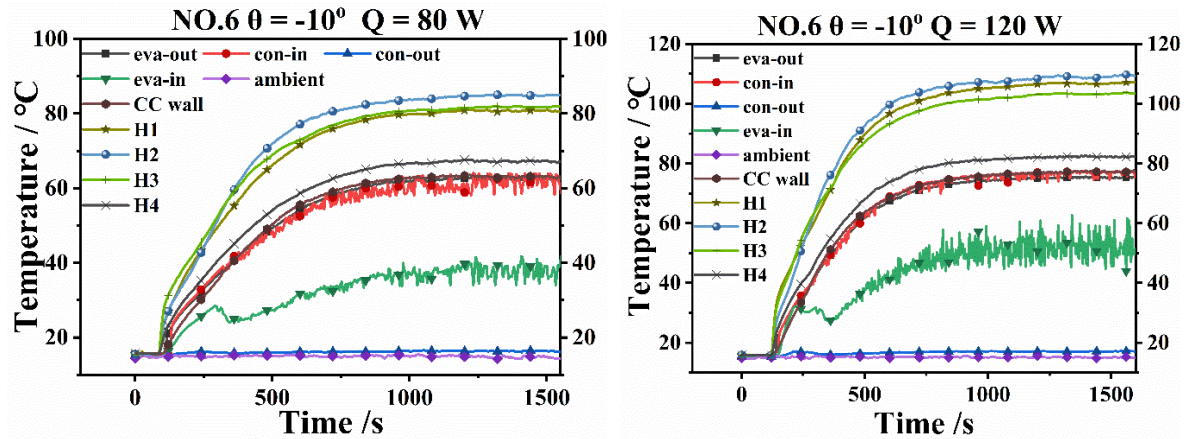


Figure 13. Temperature response during start up process of No.6 position at 80 W and 120 W.

The evaporator inlet temperature fluctuated greatly. The evaporator inlet pipeline was above the compensation chamber, so there were temperature fluctuations at the evaporator inlet, which was caused by the discontinuous liquid flow.

#### 4.5. Operation with Variable Heat Load

To investigate the stability of the LHP with direct pouring wick, the system was tested with variable heat loads under No.5 position. The ambient temperature was 19 °C and the LHP showed good adaptability to the change of heat load, but there were also temperature fluctuations during the test, especially the evaporator inlet temperature. The temperature of evaporator kept good consistency except for the heating surface. Due to the discontinuous flow of liquid, temperature fluctuations were easy to occur at the inlet of evaporator, which was more obvious with medium heat load.

Figure 14 showed the temperature characteristics of the uniform variable heat load cycle test between 20 W and 160 W. The heat load increased from 40 W to 160 W, and then decreased to 20 W by the same amplitude. Temperature overshoot occurred at 40 W and 60 W, and it decreased with the increase of heat load. When the heat load increased to 40 W and 60 W, the system was not in supercooling state. This meant the vapor line had been filled with vapor, so the temperature overshoot phenomenon was relatively smooth.

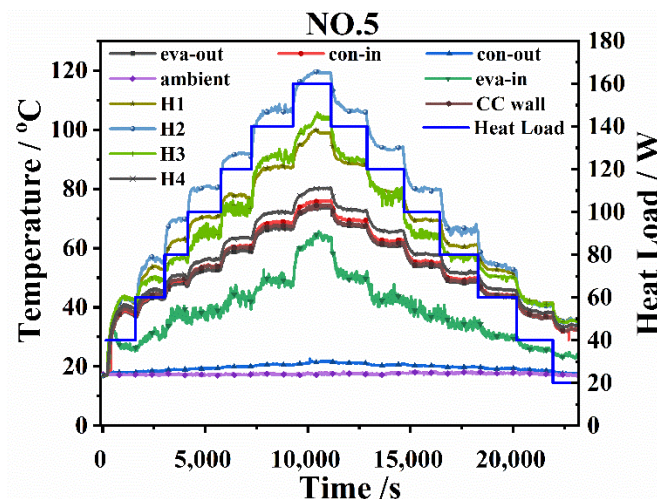


Figure 14. Temperature response during continuous operation of No.5 position at 20 W-160 W-20 W.

It was worth noting that when the heat load was 40 W, 80 W, 120 W, and 160 W, after the system was stable, the temperatures were all higher than that of the fixed heat load start up experiment under the same heat load. The analysis showed that it was related to the initial conditions of the system. The distribution of temperature and working fluid in the system affected the start up and operation of the LHP. The initial temperature of the system could be regarded as the ambient temperature, and the liquid was in the region of low gravitational potential energy. During variable heat load operation, the temperature distribution and working fluid flow state of the system in the previous stage were different from those at ambient temperature, which led to the higher temperature after reaching a new equilibrium. That also meant the stability point of the system was affected by the process. In practical applications, it is instructive to determine the thermal load corresponding to the allowable temperature of the system [8].

As mentioned above, the LHP of the No.4 position operated in reverse when starting at a low heat load. This situation also appeared in the variable heat load test, such as A and B stages in Figure 15. It was related to the relative position and heat load of the system. The experimental results showed that the reverse flow was more likely to occur in high heat load start up process under No.3 and No.4 positions. However, the condition of the No.5 position was not conducive to reverse flow, and reverse flow occurred only in the low heat load stage (10–40 W).

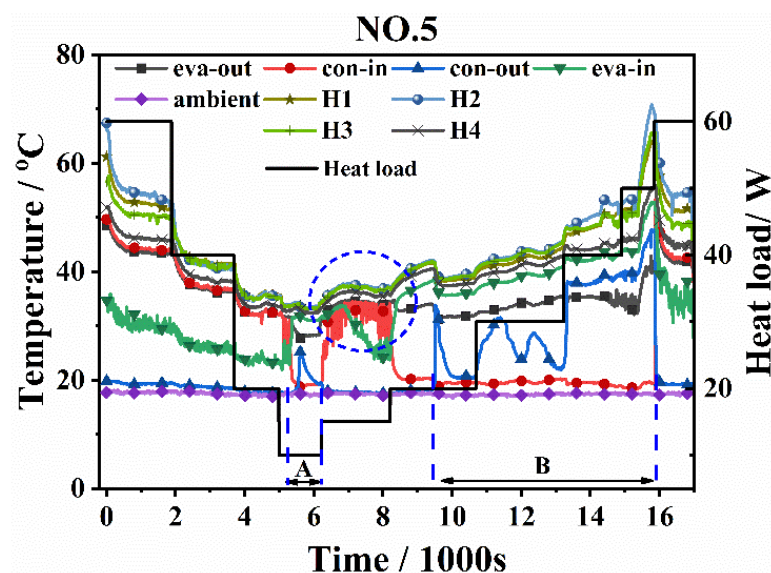


Figure 15. Temperature response during continuous operation of No.5 position at 60 W-10 W-60 W.

#### 4.6. Thermal Resistance Analysis

Thermal resistance is a significant performance index, which reflects the heat transfer ability of LHP.  $R_{LHP}$  indicates the ability of the system to absorb and discharge heat.  $R_{eva}$  reflects the performance of the porous wick in the evaporator.  $R_{con}$  represents the ability of the condenser to transfer heat to the environment.

As shown in Figure 16,  $R_{LHP}$  and  $R_{con}$  decreased with the increase of heat load. The lowest  $R_{LHP}$  was  $0.195\text{ }^{\circ}\text{C}/\text{W}$  and the lowest  $R_{con}$  was  $0.185\text{ }^{\circ}\text{C}/\text{W}$ . Due to the large area of evaporator, the evaporation area and heat capacity of the porous wick were also large, so the heat loads were all within the heat transfer limit of the system.  $R_{eva}$  was between  $0.037\text{--}0.050\text{ }^{\circ}\text{C}/\text{W}$ . The value of  $R_{eva}/R_{LHP}$  was kept at a low level, about 20%. The LHP fabricated by Deng et al. [8] was similar to this article's. They used metal wire mesh as porous wick and the value of  $R_{eva}/R_{LHP}$  was 55% at 40 W and 23% at 120 W. The comparison showed that the  $R_{eva}/R_{LHP}$  of pouring porous wick is lower than metal wire mesh wick at low heat load and more insensitive to the change of heat load.

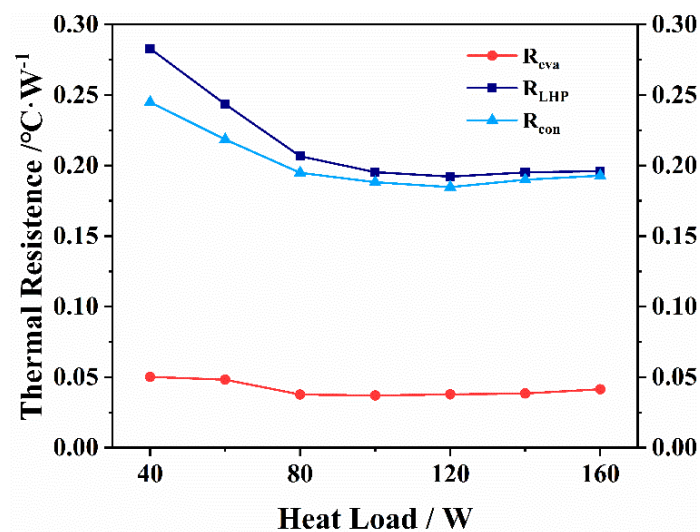


Figure 16. Thermal resistance at different heat loads of NO.5 position.

Compared with evaporator thermal resistance, the LHP thermal resistance was larger, especially at low heat loads. The reason was that when the heat load was low, the working fluid's circulation rate and mass flow rate were small. As a result, there was liquid fluid in the vapor grooves of the evaporator. With the increase of heat load, the working fluid evaporated more quickly in the vapor grooves, so that the circulation rate of the system increased. Therefore, the thermal resistance of LHP was reduced. So there is more research significance to improve the low thermal resistance working range of the system [8].

## 5. Conclusions

In this article, the advantages and technology of direct pouring porous wick for LHP were introduced. This paper provided a creative idea of setting a unique circumferential structure on the evaporator to achieve a good sealing performance of pouring porous wick. Based on this, the LHP system was fabricated and the experiments under several positions were carried out. A few conclusions were obtained from the results as follows:

- (1) The LHP system could operate stably in normal position and achieve good temperature control effect. The maximum heat load could reach 160 W. It also could operate stably under unfavorable conditions of gravity.
- (2) When the vapor grooves of LHP were located above the compensation chamber, the system was difficult to stabilize. By adding gravity assistance, the LHP could start up at 80 W and 120 W, but there would be reverse flow.
- (3) In continuous operation, the LHP showed good adaptability to the change of heat load. However, there were temperature fluctuations during the test. When the heat load was low, the reverse flow occurred.
- (4) The thermal resistance of the system decreased with the increase of the heat load, but the thermal resistance of the evaporator almost unchanged, which indicated that the pouring porous wick in the evaporator had good heat load matching.
- (5) In the future, the experimental research of direct pouring LHP should improve performance by reducing the area of evaporator and adding secondary porous wick in liquid line. Direct pouring LHP will obtain more applications because of its low cost, short manufacturing cycle and good sealing performance.

**Author Contributions:** Conceptualization, W.D., B.C. and W.L.; methodology, W.D.; investigation, T.W. (Tong Wu); resources, T.W. (Tingting Wang); data curation, Z.M.; writing—original draft preparation, B.C.; writing—review and editing, Z.L.; project administration, Z.L.; funding acquisition, Z.L. and L.M. All authors have read and agreed to the published version of the manuscript.

**Funding:** This research was funded by the National Natural Science Foundation of China, grant number 51776079 & 52076088; Project of Youth Innovative Talents in Higher Education Institutions of Guangdong, grant number 2020KQNCX069; Natural Science Foundation of Top Talent of SZTU, grant number 2019010801008.

**Institutional Review Board Statement:** Not applicable.

**Informed Consent Statement:** Not applicable.

**Data Availability Statement:** Not applicable.

**Conflicts of Interest:** The authors declare no conflict of interest.

## Nomenclature

$\lambda$	thermal conductivity, W/(m·K)
$\varepsilon$	porosity
L	length, mm
W	width, mm
H	height, mm
O	outside diameter, mm
I	inside diameter, mm
$\theta$	tilt angle, °
p	pressure, Pa
Q	heat load, W
A	heat area, cm <sup>2</sup>
q	heat flux, W/cm <sup>2</sup>
T	temperature, °C
R	thermal resistance, °C/W
Subscripts	
E	effective
S	solid metal
cap	capillary force
vl	vapor line
ll	liquid line
g	gravity
LHP	loop heat pipe
eva	evaporator
con	condenser
e	evaporator wall
e,out	evaporator outlet
e,in	evaporator inlet
c	average of condenser inlet and outlet
con, in	condenser inlet
con, out	condenser outlet
a	ambient
CC	compensation chamber

## References

- Riehl, R.; Dutra, T. Development of an experimental loop heat pipe for application in future space missions. *Appl. Therm. Eng.* **2005**, *25*, 101–112. [\[CrossRef\]](#)
- Basha, M.S.; Bansal, L.; Sarma, D.; Basu, S.; Kumar, P.; Ambirajan, A. Solar Thermal Power System Augmented with LHP. *Energy Procedia* **2014**, *49*, 295–304. [\[CrossRef\]](#)
- Hong, S.; Zhang, X.; Wang, S.; Zhang, Z. Experiment study on heat transfer capability of an innovative gravity assisted ultra-thin looped heat pipe. *Int. J. Therm. Sci.* **2015**, *95*, 106–114. [\[CrossRef\]](#)
- He, S.; Zhou, P.; Ma, Z.; Deng, W.; Zhang, H.; Chi, Z.; Liu, W.; Liu, Z. Experimental study on transient performance of the loop heat pipe with a pouring porous wick. *Appl. Therm. Eng.* **2020**, *164*, 114450. [\[CrossRef\]](#)
- Wang, Y.; Cen, J.; Jiang, F.; Cao, W.; Guo, J. LHP heat transfer performance: A comparison study about sintered copper powder wick and copper mesh wick. *Appl. Therm. Eng.* **2016**, *92*, 104–110. [\[CrossRef\]](#)
- Zhou, W.; Ling, W.; Duan, L.; Hui, K.S. Development and tests of loop heat pipe with multi-layer metal foams as wick structure. *Appl. Therm. Eng.* **2016**, *94*, 324–330. [\[CrossRef\]](#)

7. Zhang, Z.; Zhao, R.; Liu, Z.; Liu, W. Application of biporous wick in flat-plate loop heat pipe with long heat transfer distance. *Appl. Therm. Eng.* **2021**, *184*, 116283. [[CrossRef](#)]
8. Xiao, B.; Deng, W.; Ma, Z.; He, S.; He, L.; Li, X.; Yuan, F.; Liu, W.; Liu, Z. Experimental investigation of loop heat pipe with a large squared evaporator for multi-heat sources cooling. *Renew. Energy* **2020**, *147*, 239–248. [[CrossRef](#)]
9. Ren, C. Parametric effects on heat transfer in loop heat pipe's wick. *Int. J. Heat Mass Transf.* **2011**, *54*, 3987–3999. [[CrossRef](#)]
10. Hu, Z.; Wang, D.; Xu, J.; Zhang, L. Development of a loop heat pipe with the 3D printed stainless steel wick in the application of thermal management. *Int. J. Heat Mass Transf.* **2020**, *161*, 120258. [[CrossRef](#)]
11. Li, X.; Yao, D.; Zuo, K.; Xia, Y.; Zeng, Y.-P. Effects of pore structures on the capillary and thermal performance of porous silicon nitride as novel loop heat pipe wicks. *Int. J. Heat Mass Transf.* **2021**, *169*, 120985. [[CrossRef](#)]
12. Guo, H.; Ji, X.; Xu, J. Enhancement of loop heat pipe heat transfer performance with superhydrophilic porous wick. *Int. J. Therm. Sci.* **2020**, *156*, 106466. [[CrossRef](#)]
13. Li, H.; Liu, Z.; Chen, B.; Liu, W.; Li, C.; Yang, J. Development of biporous wicks for flat-plate loop heat pipe. *Exp. Therm. Fluid Sci.* **2012**, *37*, 91–97. [[CrossRef](#)]
14. Zhou, G.; Li, J.; Jia, Z. Power-saving exploration for high-end ultra-slim laptop computers with miniature loop heat pipe cooling module. *Appl. Energy* **2019**, *239*, 859–875. [[CrossRef](#)]
15. Zhou, W.; Li, Y.; Chen, Z.; Deng, L.; Gan, Y. A novel ultra-thin flattened heat pipe with biporous spiral woven mesh wick for cooling electronic devices. *Energy Convers. Manag.* **2019**, *180*, 769–783. [[CrossRef](#)]
16. He, S.; Liu, Z.; Wang, D.; Liu, W.; Yang, J. Effect of different charge ratios on transient performance of a flat type of the LHP with a shared compensation chamber. *Int. J. Heat Mass Transf.* **2019**, *138*, 1075–1081. [[CrossRef](#)]
17. Tian, W.; He, S.; Liu, Z.; Liu, W. Experimental investigation of a miniature loop heat pipe with eccentric evaporator for cooling electronics. *Appl. Therm. Eng.* **2019**, *159*, 113982. [[CrossRef](#)]
18. Wu, S.-C.; Wang, D.; Chen, Y.-M. Investigating the effect of double-layer wick thickness ratio on heat transfer performance of loop heat pipe. *Int. J. Therm. Sci.* **2014**, *86*, 292–298. [[CrossRef](#)]